CHAPTER 31

MEASUREMENT OF BED SHEAR STRESS UNDER WAVES

H.P. Riedel[1], J.W. Kamphuis[2] and A. Brebner[3]

ABSTRACT

Shear stress measurements on both smooth and sand roughened beds were carried out in an oscillating water tunnel using a flexurally supported shear plate. The range of simulated wave boundary layers covered practically any situation possible in the field or laboratory.

In the laminar range good agreement is obtained with the theoretical shear stress calculated from first order wave theory. However, in the turbulent flow regimes the experimental data indicates that theory results in an overestimate of the shear force by 20-50%. Limits of laminar, smooth turbulent and rough turbulent flow regimes are determined and it appears that the rough turbulent flow regime may itself be subdivided into two sections, each having different turbulence characteristics.

INTRODUCTION

Many researchers have devoted their time in recent years to the study of waves in flumes, model basins and in the field, but the state of knowledge on the interaction of waves and the bed is still limited. A better understanding of the oscillatory boundary layer at the bed is necessary because most shallow water wave phenomena are largely influenced by bottom friction.

For any study of the oscillatory boundary layer a means of generating the wave boundary layer must be found and appropriate tools are needed to measure the relevant boundary layer parameters. An oscillating water tunnel was built to satisfy the first requirement and both prototype and model scale wave boundary layers could be simulated. With respect to measurement, the most useful boundary layer parameter is

---

1. Research Associate,

2. Associate Professor of Civil Engineering,

3. Professor and Head of Civil Engineering,

Coastal Engineering Research Laboratory, Queen's University at Kingston Canada.

velocity, however, velocity meters which do not disturb the flow and which are capable of measuring the unsteady flow within thin boundary layers are only now being developed. Consequently, an alternative parameter, bed shear stress, was measured by a shear stress transducer which did not interfere with the boundary layer flow.

To date experimental methods of determining shear stress have only yielded a limited amount of data e.g. Bagnold (1), Iwagaki et al (2), Inman & Bowen (3), Jonsson (4), Yalin & Russel (5), and Teleki & Anderson (6). As a result, theoretical expressions for shear stress at the bed outside the laminar range, as given by Jonsson (4) and Kajiura (7), have not been adequately verified experimentally.

EXPERIMENTAL EQUIPMENT

Wave boundary layers were simulated in an oscillating water tunnel illustrated in figure 1. The construction is all concrete and glass which gives minimum leakage and a maximum viewing area in the working section. The working section is 12 m long, 1 m high and 0.5 m wide. Nine 13 mm thick plate glass windows (.9 m x 1 m) on each side allow a clear view throughout the working section. Access to the working section is provided by hatches located above each window.

A 2 m square piston moves the water with periods ranging from 2.5 to 15 seconds and strokes up to 1 m. With an 8:1 reduction in cross-sectional area between the piston "bore" and the working section, orbital diameters of 8 m in length are possible in the working section. The honeycombs at the entrance to the working section straighten the flow and prevent large scale eddies, which may be generated in the bends, from entering the working section. The sediment trap prevents granular material from reaching the piston and fouling it.

A 18.7 KW Reeves Varispeed motor drives the piston through a 31.4:1 Philadelphia reducer giving a continuously variable output speed range of 4.3 - 56.5 R.P.M. The output shaft of the gearbox drives a crank arm with an eccentricity that may be adjusted from 0-0.5 m. Then a connecting rod and shaft transfer this motion to the piston.

Superimposed unidirectional currents may be added by means of a

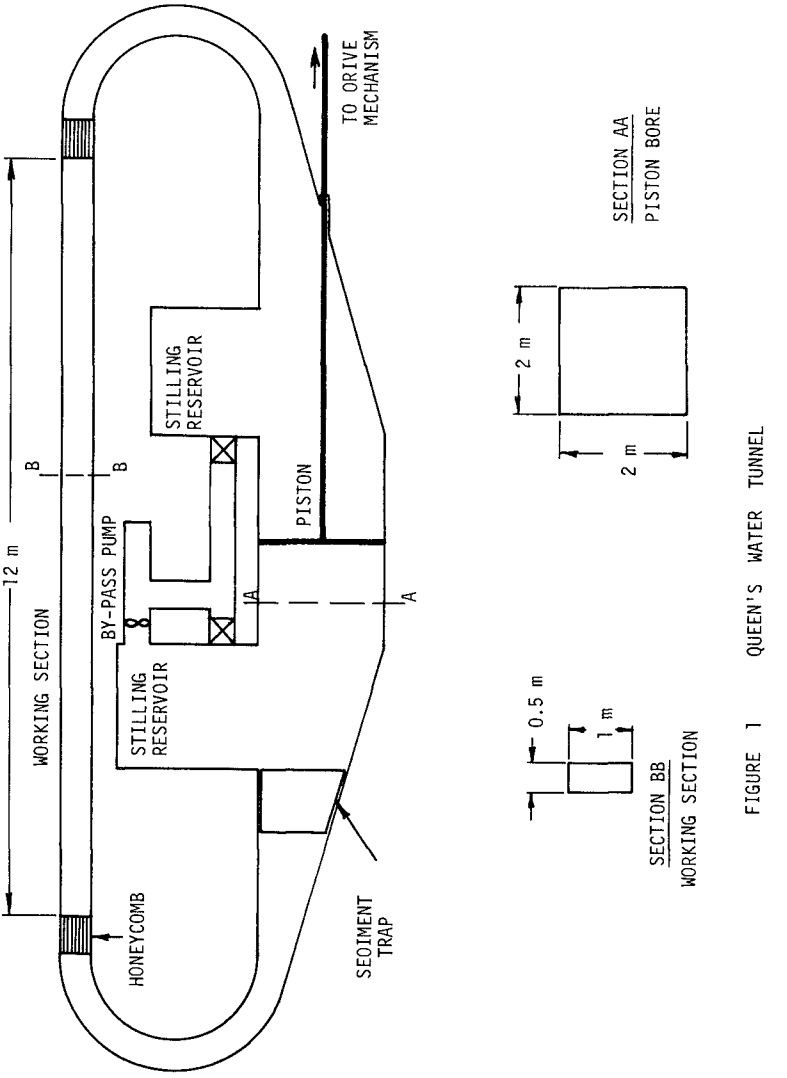

FIGURE 1 QUEEN'S WATER TUNNEL

by-pass pump. The stilling reservoirs are included to dampen the turbulence resulting from the pump discharge.

Shear stress was measured using the shear plate shown as a centre-line section in figure 2. The rectangular shear sensitive plate (6), 0.048 square metres in surface area, is mounted inside an outer plate (1) so that in its equilibrium position there is a gap of 1 mm at each end through which the plate can deflect. Clearance gaps of 0.5 mm are provided at the sides of the plate. The position of the shear plate can be adjusted by the fastening blocks (2, 11). Similar blocks not seen in the view of figure 2 locate the shear plate laterally. In this way the level of the shear sensitive surface can be adjusted to match the outer plate within 0.1 mm.

The shear plate is supported at its corners by 4 thin stainless steel legs (4) which are clamped to the base plate (12, 13) and bonded to the shear sensitive plate. A buffer plate (8) and flow interruptor (7), impede the flow of secondary currents under the shear plate. Pressure tappings P_1, P_2, P_3 and P_4 monitor the pressure in the freestream as well as under the shear plate. With this system both end pressure forces, which act on the leading and trailing edges of the plate, and vertical pressure forces can be determined. The apparent measured shear is then corrected for these forces. The 1.65 mm thick stainless steel plate is stiffened longitudinally by two 6.5 mm square bars fitted onto the bottom edges (9). This arrangement gives a relatively small frontal area but is still stiff enough to prevent bowing of the shear plate under vertical loading.

Strain gauges mounted in pairs on the upstream support legs sense any deflection of the shear plate and a temperature compensated full bridge circuit is used which gives a linear output over the full-scale range of shear ($\pm 100 N/m^2$). The shear plate output is stable for sensitivities as low as $0.015 N/m^2$.

A complete flushing system was installed to cope with loose sand grains and any other dirt in the tunnel. The outer plate assembly provides a four walled enclosure within which the shear plate is located. Water under mains pressure can be fed into this enclosure via flushing pipes (10, 15) and a third one not seen in figure 2. The only way the water can escape is through the gaps around the shear

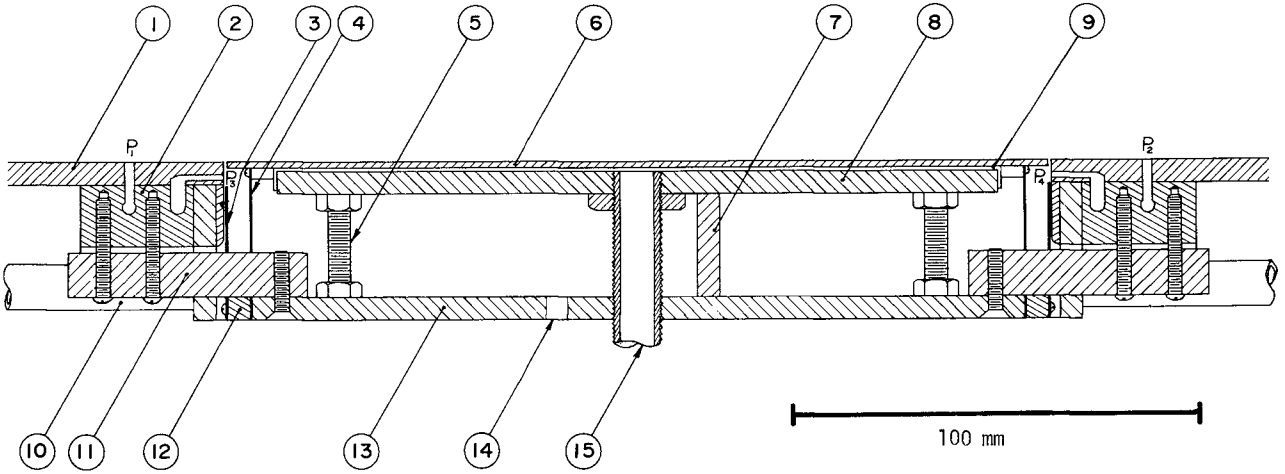

1 OUTER PLATE
2 SHEAR ASSEMBLY OUTER FASTENING BLOCK
3 DEFLECTOR
4 STAINLESS STEEL FLEXURE LEGS
5 BUFFER PLATE ADJUSTING SCREWS
6 SHEAR PLATE
7 FLOW INTERRUPTOR
8 BUFFER PLATE
9 SHEAR PLATE STIFFENER
10 END FLUSHING PIPE
11 SHEAR ASSEMBLY INNER FASTENING BLOCK
12 CLAMPING BAR
13 BASE PLATE
14 STRAIN GAUGE WIRING OUTLET
15 BUFFER FLUSHING PIPE

FIGURE 2 SHEAR PLATE ASSEMBLY

plate and so a jet-like flushing system is established.

Sand roughened beds as illustrated in figure 3, were used. Table 1 lists the equivalent sand roughness k_s for each of the surfaces.

TABLE 1. Equivalent sand roughness data

Material No.	D_{50}(mm)	D_{90}(mm)	k_s(mm)
1	0.37	0.50	1.41
2	1.65	2.20	8.43
3	3.13	4.22	15.8
4	9.8	12.3	51.5
5	50	50	139

EXISTING SHEAR STRESS THEORIES

Over the laminar range use of first order wave theory and solution of the resultant boundary layer equation, (e.g. Jonsson (4)) yields

$$\hat{\tau} = \rho \hat{U}_\delta^2 / \sqrt{RE} \qquad (1)$$

where $\hat{\tau}$ is the maximum shear stress at the bed, ρ the density of water, $\hat{U}_\delta$ the maximum orbital velocity just outside the boundary layer and RE the maximum amplitude Reynolds number for sinusoidal motion which is equal to $\hat{U}_\delta a_\delta / \nu$ where a_δ is the orbital amplitude just outside the boundary layer and ν the kinematic viscosity of water.
Eq. 1 may be rewritten as

$$f_w = \frac{2}{\sqrt{RE}} \qquad (2)$$

where $f_w = 2\hat{\tau}/\rho \hat{U}_\delta^2$, a wave friction factor as defined earlier by Jonsson (4).

Expressions for wave friction factor, or shear stress have been theoretically derived in the smooth turbulent and rough turbulent flow regimes by Kajiura (7). The derivation followed along the lines of

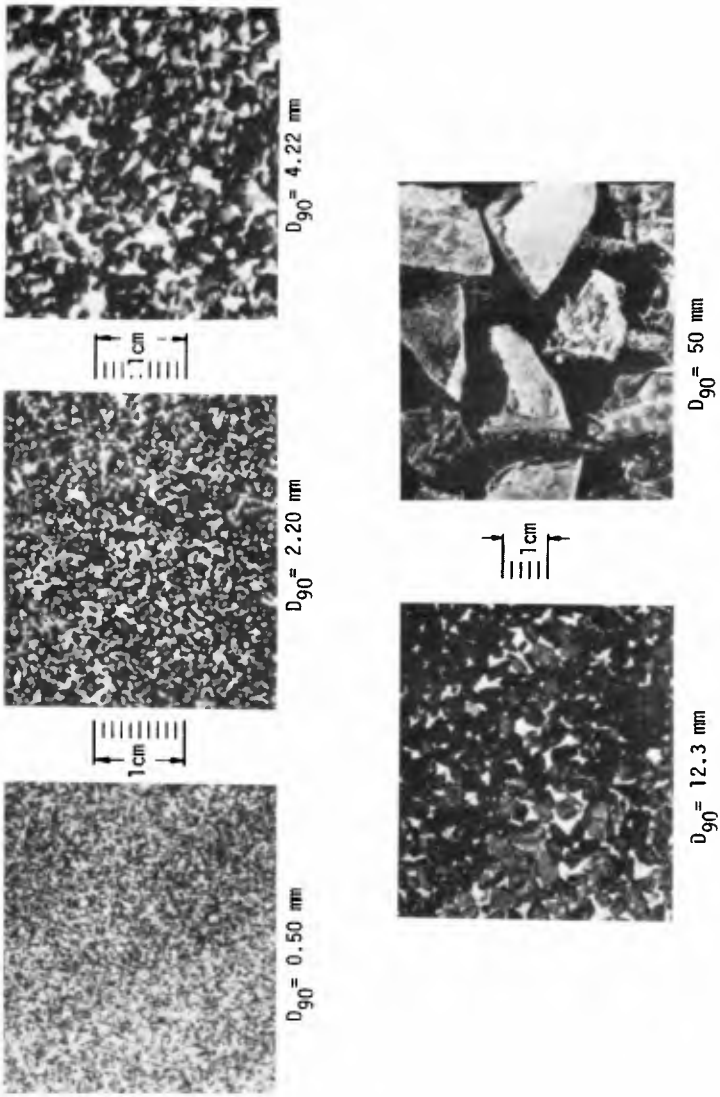

FIGURE 3 ROUGH BEDS

unidirectional turbulent boundary layer theory as presented by Mellor & Gibson (8). In this approach the boundary layer was sub-divided into inner, overlap and outer layers and for each of these a different form of eddy viscosity was assumed. The boundary layer equations were then solved. However, the theory has its limitations because it assumes an average state of turbulence over the wave period. Also constants evaluated from unidirectional flow measurements are used. On the other hand a better theoretical formulation cannot be developed until detailed velocity studies within the boundary layer have been completed.

For the smooth turbulent flow regime Kajiura obtained

$$\frac{1}{8.1\sqrt{f_w}} + \log \frac{1}{\sqrt{f_w}} = -0.135 + \log \sqrt{RE} \qquad (3)$$

Over rough beds Kajiura gives

$$\frac{1}{4.05\sqrt{f_w}} + \log \frac{1}{4\sqrt{f_w}} = -0.254 + \log \frac{a_\delta}{k_s} \qquad (4)$$

Jonsson (4) deduced a similar expression based on the measurement of velocity profiles of one wave simulated in a water tunnel.

$$\frac{1}{4\sqrt{f_w}} + \log \frac{1}{4\sqrt{f_w}} = -0.08 + \log \frac{a_\delta}{k_s} \qquad (5)$$

RESULTS

For the smooth bed and for each of the sand roughened beds, from 37 to 63 shear measurements were made over the Reynolds number range $300 < RE < 5.5 \times 10^6$. The measured shear stress and pressure differences between the various tapping points were recorded on chart paper and from there the data was transferred to punched cards. In this way corrections were made to the recorded shear(i) for end pressure forces resulting from the pressure difference across the shear plate and the roughness elements glued to it, (ii) for vertical pressure loading which resulted because the freestream pressure was not being transmitted under-

neath the plate and (iii) for vertical dead-weight loading of the roughness elements. (i) Depends only on the frontal area of the plate, roughness size and packing,and the pressure gradient. The effects of (ii) and (iii) also depend on the magnitude of the shear stress which deflects the plate in the direction of the flow. i.e. the deflection of the plate from its mean position will influence its response to a vertical load.

Using this method of analysis, the maximum shear stress was obtained for each record and the wave friction factor calculated. The results are presented in the form of a wave friction factor diagram where f_w is plotted against RE. This diagram has a similar format to the Stanton diagram for pipe flow. Jonsson (4) first presented a diagram of this form but it was based on very little data. The data obtained in the present experiments is sufficient to define the wave friction factor diagram over the range of practical use.

Figure 4 shows the experimentally determined wave friction factor diagram. For ease of interpretation this figure 4 has been reproduced in figure 5 with the data points omitted. Inspection of these figures shows:

(a) Within the laminar range the agreement between theory and experiment is very good. This agreement indicates that the shear plate operation was satisfactory and that the corrections for secondary forces were adequate.

(b) The upper limit of the laminar range occurs for RE $\simeq 10^4$ which corresponds approximately to the middle of the observed range of values of transition for wave flume and oscillating plate tests. However, the transition in wave flumes and on oscillating plates was determined by observation of dye streaks. The conclusions drawn for these depend largely on the observer's interpretation.

(c) In the smooth turbulent range the data points define a curve which lies 25-30% below that predicted by Kajiura (7). This difference is remarkably small considering the assumptions that were made in the derivation of the theoretical expression. The lower limit of the smooth turbulent regime was found to be RE = 6×10^5. This corresponds quite well with that derived by Kajiura.

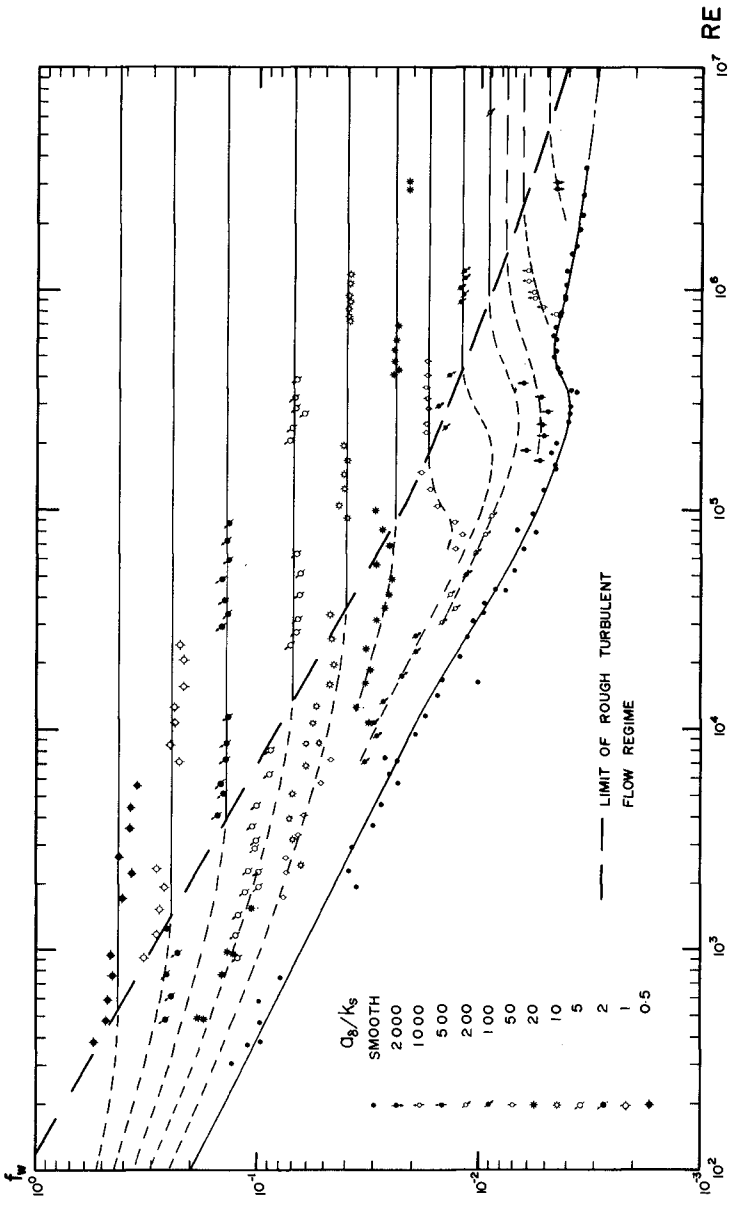

FIGURE 4 EXPERIMENTAL WAVE FRICTION FACTOR DIAGRAM

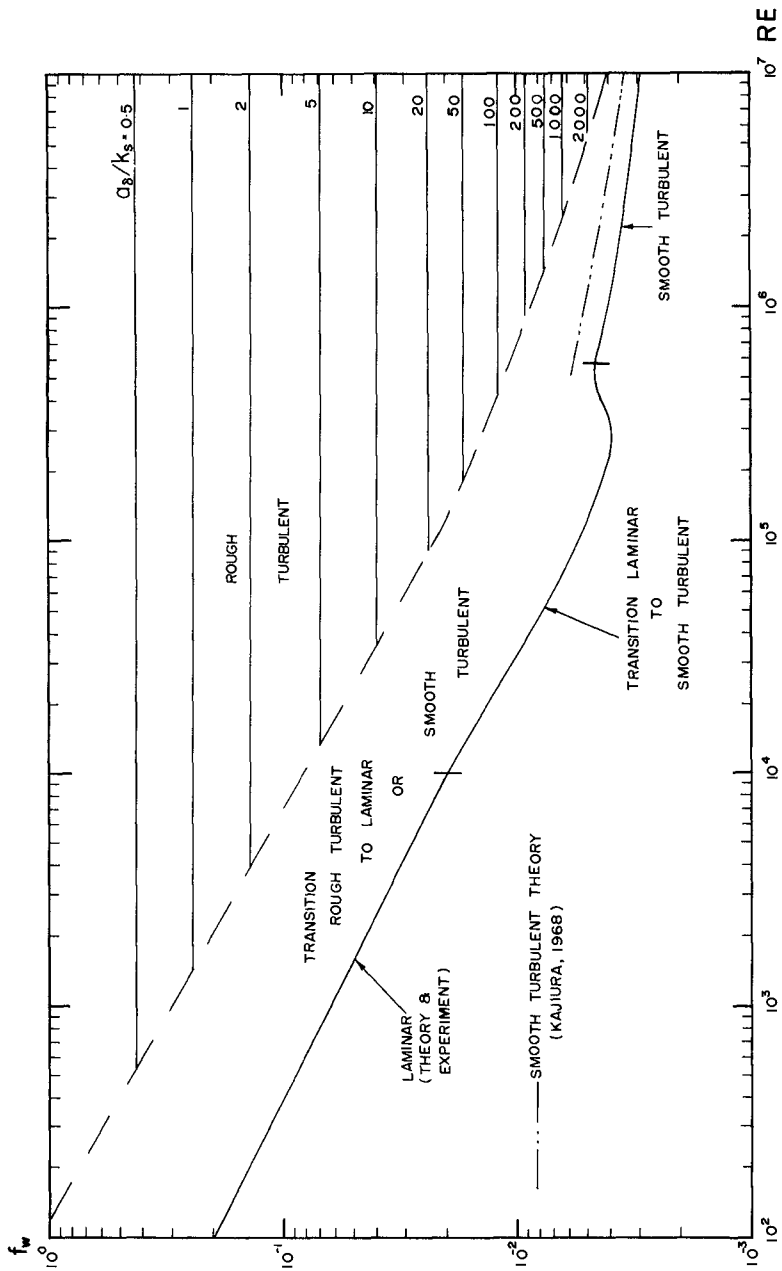

FIGURE 5 WAVE FRICTION FACTOR DIAGRAM SHOWING FLOW REGIMES AND THEORETICAL CURVES.

(d) The lower limit of the rough turbulent regime is defined by the dashed line which was drawn through the points where the family of a_δ/k_s lines curves away from the horizontal (in the rough turbulent regime the friction factor is independent of RE). This lower limit may be expressed in terms of the roughness Reynolds number $k_s v_*/\nu$ (Table 2). It may be seen that for $a_\delta/k_s < 25$, $k_s v_*/\nu$ has a constant value of approximately 500. As a_δ/k_s becomes larger $k_s v_*/\nu$ becomes smaller and it would be expected that as $a_\delta/k_s \to \infty$, $k_s v_*/\nu \to 70$ as for unidirectional flow. Values of other commonly used transition parameters $k_s \hat{U}_\delta/\nu$ and k_s/δ_L have been included in Table 2 for completeness.

(e) In the transition region between rough turbulent flow and laminar or smooth turbulent flow the data points tend to be less ordered. The parameter k_s has because of its definition been measured in the rough turbulent flow regime, and consequently its physical significance is restricted to that regime. In the transition region the flow is a function of the shape of the individual roughness elements and their packing density and not a known function of k_s. Hence these curves must be used with caution within the transition flow regime.

The data for the rough turbulent frow regime has been replotted as f_w against a_δ/k_s since RE is no longer important. (Figure 6). Using a least squares fitting technique, the following equation results

$$\frac{1}{4.95\sqrt{f_w}} + \log \frac{1}{4\sqrt{f_w}} = 0.122 + \log \frac{a_\delta}{k_s} \qquad (6)$$

This equation is consistent with the assumption that a logarithmic velocity law exists near the bed. For $a_\delta/k_s > 25$ the actual data points are in good agreement with this curve. Here the orbital amplitudes are relatively large and as $a_\delta/k_s \to \infty$ unidirectional flow is approached. Also the phase difference between the freestream velocity and the shear stress at the bed approaches zero as $a_\delta/k_s \to \infty$. So it may be concluded

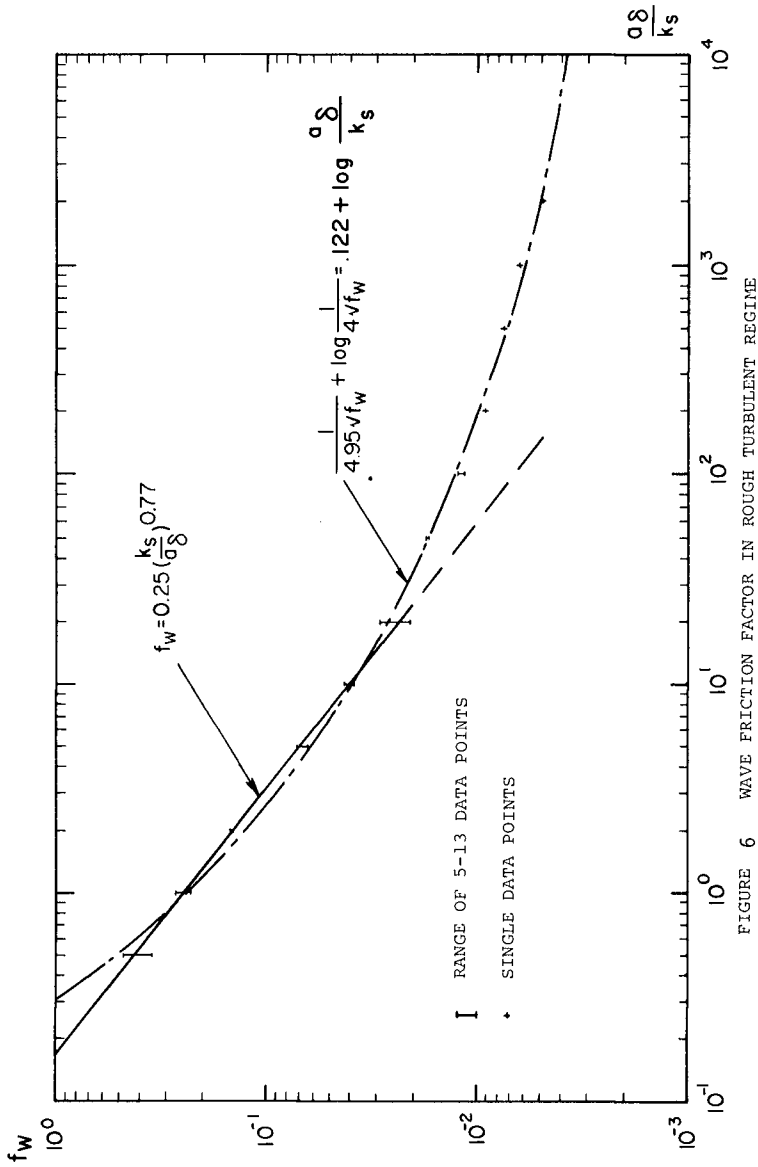

FIGURE 6 WAVE FRICTION FACTOR IN ROUGH TURBULENT REGIME

that the assumption of a logarithmic velocity profile at the instant of maximum freestream velocity is reasonable.

TABLE 2. Lower limits of rough turbulent flow regimes.

$\frac{a_\delta}{k_s}$	$\frac{k_s v_*}{\nu}$	$\frac{k_s \hat{U}_\delta}{\nu}$	$\frac{k_s}{\delta_L}$
0.5	490	1060	32.5
1	490	1400	26.4
2	512	1925	21.9
5	487	2600	16.1
10	495	3500	13.1
20	487	4450	10.6
50	325	3500	5.92
100	340	4400	4.70
200	290	4300	3.30
500	170	2700	1.65
1000	135	2350	1.08
2000	135	2700	0.82

For $a_\delta/k_s < 25$ the data points deviate systematically from the curve defined by equation 6. This results from a large phase difference between the shear stress at the bed and the freestream velocity ($\simeq 45^o$) and this phase difference has a controlling influence on the boundary layer velocity profile. i.e. the velocity profile is not logarithmic near the bed. For $a_\delta/k_s < 25$ the data points fit very closely on a straight line given by

$$f_w = 0.25 \left(\frac{k_s}{a_\delta} \right)^{0.77} \qquad (7)$$

It is then recommended that equation 7 be used to calculate friction factor or bed shear in the rough turbulent regime for $a_\delta/k_s < 25$ and

equation (6) be used for $a_\delta/k_s > 25$. Jonsson's (4) and Kajiura's (7) curves are included in figure 7 for comparison. It may be seen that Kajiura's predicted friction factor is 30-50% higher than the experimentally determined line, while Jonsson's curve falls 20-40% above the line. Experimentally determined wave friction factors in the rough turbulent regime by Bagnold (1) and Inmann and Bowen (3) fall between the experimental curve and Jonsson's curve.

CONCLUSIONS

Direct measurement of bed shear stress was attempted for a wide range of oscillatory flows produced in a water tunnel. The following conclusions were reached.

1. A wave friction factor diagram similar to the Moody diagram for unidirectional flow was obtained experimentally. The parameters a_δ and T for a wave motion over a bed of roughness, k_s, define the flow regime within the boundary layer and allow the maximum shear stress at the bed to be computed.

2. Transition between flow regimes may be expressed in terms of numerical values of the Reynolds numbers RE and $k_s v_*/\nu$. For a smooth bed the upper limit of the laminar flow regime occurs at $RE = 9\times10^3$ while the lower limit of the smooth turbulent regime occurs at $RE = 6\times10^5$. For rough beds with $0.1 < a_\delta/k_s < 25$ the lower limit of the rough turbulent flow regime is given by $k_s v_*/\nu = 500$. As a_δ/k_s becomes larger the value of $k_s v_*/\nu$ at transition reduces so that as $a_\delta/k_s \to \infty$, $k_s v_*/\nu \to 70$.

3. In the rough turbulent flow regime the wave friction factor may be expressed as

$$f_w = 0.25 \left(\frac{k_s}{a_\delta} \right)^{0.77} \quad ; \quad 0.1 < a_\delta/k_s \leq 25$$

$$\frac{1}{4.95\sqrt{f_w}} + \log \frac{1}{4\sqrt{f_w}} = 0.122 + \log \frac{a_\delta}{k_s} \quad ; \quad a_\delta/k_s > 25$$

4. The assumption of a logarithmic velocity profile for the oscillatory boundary layer is reasonable for $a_\delta/k_s > 25$. For $a_\delta/k_s < 25$ the experimental data indicates that this assumption needs to be modified.

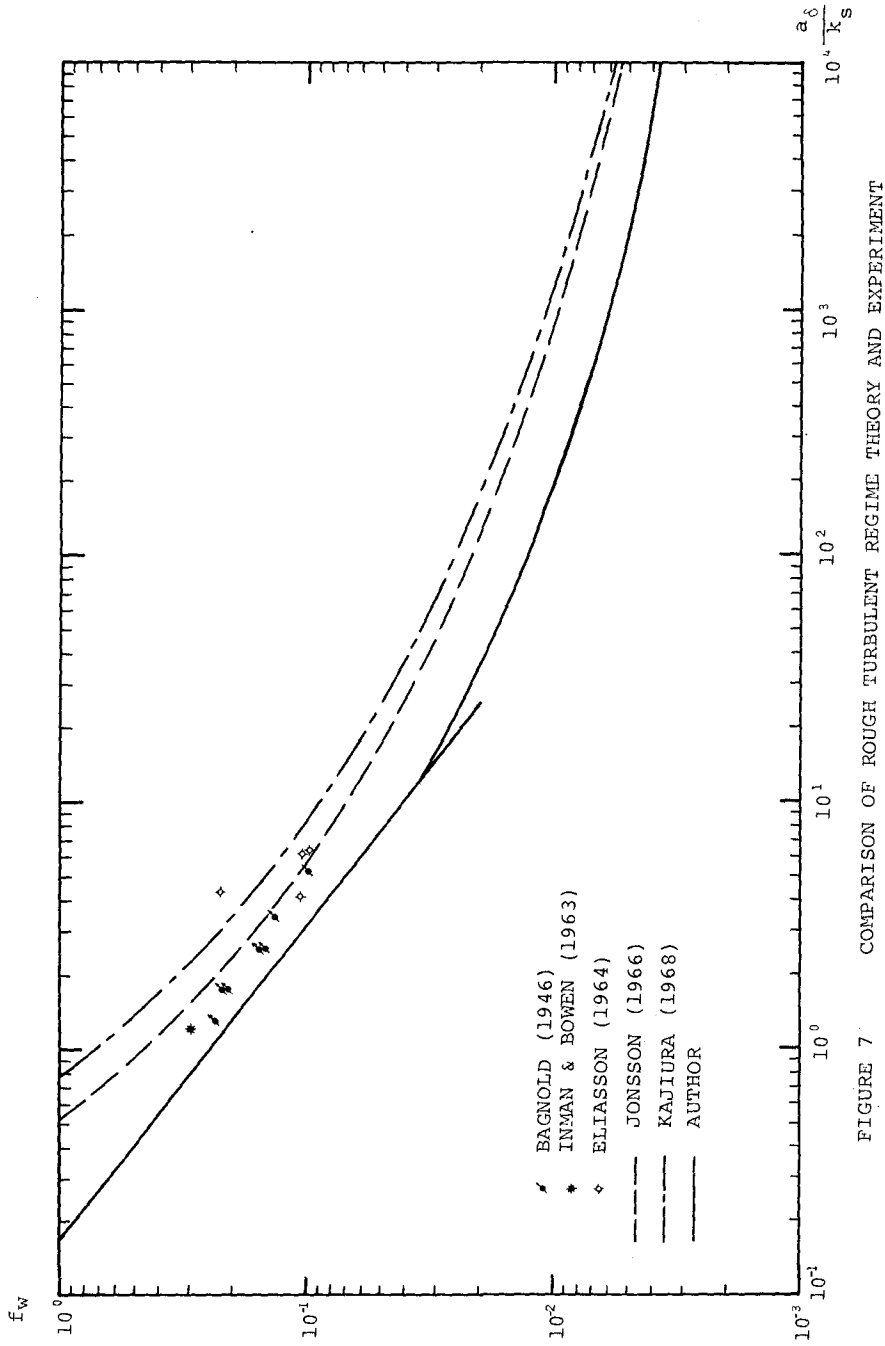

FIGURE 7 COMPARISON OF ROUGH TURBULENT REGIME THEORY AND EXPERIMENT

ACKNOWLEDGMENTS

Financial support for this program of study came from the National Research Council of Canada while the senior author was sponsored under the Canadian Commonwealth Scholarship Scheme.

REFERENCES

Bagnold, R.A. (1946) "Motion of Waves in Shallow Water. Interactions between Waves and Sand Bottoms", Proc. Roy. Soc. Lond., Series A, Vol. 187, pp 1-18.

Inman, D.L. & Bowen, A.J. (1963) "Flume Experiments on Sand Transport by Waves and Currents", Proc. of 8th Conference on Coastal Engineering, Mexico City, pp. 137.

Iwagaki, Y., Tsuchiya, Y. & Sakai, M. (1965) "Basic Studies on the Wave Damping due to Bottom Friction", Coastal Eng. in Japan, Vol. 8, pp. 37.

Jonsson, I.G. (1963) "Measurements in the Turbulent Wave Boundary Layer", 10th Congress IAHR, Lond., pp. 85.

Kajiura, K. (1968) "A Model of the Bottom Boundary Layer in Water Waves", Bull. Earthquake Res. Inst., Vol. 46, pp. 75.

Mellor, G.L. & Gibson, D.M. (1966) "Equilibrium Turbulent Boundary Layers", J. Fluid Mech., 24, pp 235.

Teleki, P.G. & Anderson, M.W. (1970) "Bottom Boundary Shear Stresses on a Model Beach ", Proc. of 12th Coastal Engineering Conference, Washington D.C., Vol. 1, pp. 269-288.

Yalin, M.S. & Russell, R.C.H. (1966) "Shear Stresses due to Long Waves", J. Hyd. Res. 4, No. 2, pp. 55.